International Conference on Lightning Protection
33rd International Conference on Lightning Protection
25 - 30 September 2016
Estoril, Portugal

Implementation and Performance Analysis of the Lightning Potential Index as a Forecasting Tool

Elisabetta Fiori, Martina Lagasio, Antonio Parodi
CIMA Research Foundation
Savona, Italy
elisabetta.fiori@cimafoundation.org

Renato Procopio
Naval, ICT and Electrical Engineering Department, University of Genoa
Genoa, Italy

Alexander Smorgonskiy, Farhad Rachidi
EMC Laboratory, Swiss Federal Institute of Technology (EPFL)
Lausanne, Switzerland

Gerhard Diendorfer
OVE Service GmbH, Dept. ALDIS
Vienna, Austria

***Abstract*— Severe weather events are responsible for hundreds of fatalities and millions of euros of damage every year in the Mediterranean basin. Lightning activity is a characteristic phenomenon of severe weather and often accompanies torrential rainfall, which under certain conditions like terrain type, slope, drainage and soil saturation can generate flash flood. Therefore, the improvement in forecast skill for those high impact weather events is one of the main challenges in early warning systems. On the line of this need the behavior of the Lightning Potential Index (LPI) is evaluated in different case studies involving complex terrain. Such index represents a measure of the potential for charge generation and separation that lead to total lightning occurrence in clouds (both IC and CG).**

Keywords-Lightning Potential Index; Lightning prediction; WRF; meteorological models; extreme events; orographic precipitation

I. INTRODUCTION

Flash floods are one of the most dangerous meteorological hazards that affect Mediterranean countries. The scientific and technical community is well aware of the rapid rising of the damages produced by flash floods [1, 2]. Therefore, it becomes very important to improve the forecast skill for those severe events. Flash floods are usually caused by intense thunderstorms accompanied by torrential rainfall that typically develops in a short range of time (1-2 hours). As a result, it is necessary to use observational and modeling data with high temporal and spatial resolution to develop methodologies to forecast thunderstorms. Strong updrafts always accompany thunderstorms and according to recent studies [3] produce large amounts of hydrometeors in the mixed ice phase region. The presence of such particles is in turn a necessary component for electrification processes that lead to lightning occurrence [4]. As a consequence, convective processes are one of the most important ingredients for the occurrence of lightning phenomenon. Thus, lightning activity can be used to map the location of the core of the thunderstorms where the heaviest rainfall is normally situated [5]. The interplay between lightning and rain evolution in thunderstorms is supported by many studies performed in different geographical locations around the globe and corresponding to different weather regimes [6-8]. Although many real-time lightning detection systems are now able to determine with high accuracy the impact location of lightning, there is a much lower capability to predict the potential for lightning occurrence in short-range forecast [9].

Lightning prediction has recently seen significant advances. The National Severe Storm Laboratory (NSSL) produces near-real-time hourly total lightning forecasting with 36 hours lead times, based on model-derived graupel flux in convective clouds with the total ice content to obtain a statistical relationship between these parameters and the total lightning flash density [10]. Some studies have formulated a forecasting methodology, allowing the identification of convective cells and related lightning phenomena in their early stages, when the “critical electric field strength” reaches a certain threshold value [11]. Recently Lynn and Yair [9,12,13] have proposed the Lightning Potential Index (LPI) that uses the direct

correlation of lightning activity with the microphysical and dynamical process within the cloud. The LPI is an empirical formula containing cloud physical parameters and is calculated within the charge separation region of clouds where the non-inductive mechanism of collision of ice and graupel particle is most effective.

While in Yair et al. [13] LPI is applied to Mediterranean case studies, in this work, the LPI is applied to the outputs of a weather forecast model (the Advanced Research Weather Research and Forecast model (WRF-ARW)) in two different areas characterized by complex terrain not only in Mediterranean areas and not all cases are characterized by extreme events. The first case study is relevant to the severe flood occurred on October 9th, 2014 in Western Italy (Liguria region), while the second benchmark case consists of six ordinary events occurred in Switzerland in different seasons. The paper is organized as follows. In Section II, the LPI definition and implementation are presented. Section III describes the WRF-ARW model setup for the considered case studies and the observed data used to validate both model and LPI performances. Section IV shows the LPI application to the different case studies. Finally, in Section V some conclusions and considerations on the obtained results are given.

II. LIGHTNING POTENTIAL INDEX (LPI)

In this section, the LPI is first defined from a physical point of view (Subsection II.A) according to [12]; then, some details on its implementation are presented (Subsection II.B).

A. Definition

The Lightning Potential Index (LPI) has been proposed by Lynn and Yair [9,12,13] to evaluate the potential for lightning activity starting from the weather forecast model outputs. They have shown that LPI correlates positively with observed lightning density and also with heavy rainfall. The LPI is a kinetic energy of the updraft [13] and measures the potential for charge generation and separation that leads to lightning flashes in the developing thundercloud. In [9], the index is defined as a volume integral of the total mass flux of ice and liquid water within a zone between 0 and -20 °C called "charging zone" where the non-inductive mechanism by collisions of ice and graupel particles in the presence of supercooled water is most effective [4,13]. The LPI has its largest values in the presence of strong vertical velocities [15] when graupel exists in equal ratios relative to snow, ice and water.

For each grid point of the 3D spatial domain of the meteorological model, a circle with a radius r of 5 grid points [9] is chosen. Then, if the majority of the grid points inside that area has a vertical velocity w greater than a threshold value w_T=0.5 [m/s] (indicating the growth phase of thunderstorm), the LPI [J/kg] can be calculated as follows:

$$LPI = \frac{1}{V}\iiint \varepsilon w^2 dxdydz \tag{1}$$

where the integral is performed on the volume V defined by the chosen area and the charging zone along the vertical axis. If this is not the case, the LPI is set to zero. The integrand function contains the vertical velocity w in [m/s] and the dimensionless number ε, which assumes values between 0 and 1, and is defined as:

$$\varepsilon = 2\frac{(Q_i Q_l)^{0.5}}{(Q_i + Q_l)} \tag{2}$$

where Q_l is the total liquid water mass mixing ratio in [kg/kg] and Q_i is the ice fractional mixing ratio in [kg/kg] defined by:

$$Q_i = q_g[((q_s q_g)^{0.5}/(q_s + q_g)) + ((q_i q_g)^{0.5}/(q_i + q_g))] \tag{3}$$

$$Q_l = q_r + q_c \tag{4}$$

where q_i is the cloud water q_r the rain water, q_g the graupel, q_s the snow and q_i the ice mixing ratio. ε is a scaling factor for the cloud updraft, and attains a maximal value when the mixing ratios of super-cooled liquid water (Q_l) and of the combined ice species (Q_i) are equal. The maximum value of ε occurring when the two ratios are equal, in accordance with the laboratory experiments summarized by Saunders [4] that have indicated that the charge separation requires all the species to operate synergistically within the charging zone.

B. Implementation

The LPI formula (1) is time dependent and is continuous in time and space. However, model data are discretized in time and space. The sampling is uniform for the horizontal direction (Δx=Δy) and for the time, while a nonuniform sampling is used for the height. Since the most important atmospheric phenomena occur in the atmospheric zone closer to the ground, a higher and not equally distributed numbers of vertical levels are generally employed in the first kilometers of the atmosphere. A smaller number of more spatially distributed vertical levels is used to discretize the remaining part of the atmosphere. Each grid point P is identified by 4 variables which are (x,y,z) for the localization in the spatial domain and t which is referred to the instant of time, so $P(x,y,z,t)$ is univocally identified. The identification of the charging zone can be done observing that the temperature T [°C] as a function of the height z is monotonically decreasing; as a consequence, for each x_i with i=1,..., N_x (the total number of grid points in the west-east direction) and y_j with j=1,..., N_y (the total number of grid points in the south-north direction), it is possible to state that:

$$\begin{cases} T = 0°C \quad at\ z_{0_{i,j}} \\ -20°C < T < 0°C \quad at\ z_{k_{i,j}}\ with\ k_{i,j} = 1,...,N_{z,i,j} \\ T = -20°C \quad at\ z_{-20_{i,j}} \end{cases} \tag{5}$$

in which $N_{z,i,j}$ is the total number of vertical levels where T is 0°C<T<-20°C at point x_i,y_j.

The implementation of the hypothesis according to which the LPI value is not zero if the majority of the points inside the chosen area around each grid point has a vertical velocity greater than the specified initial can be done as follows:

For each grid point $P(x_i,y_i,z_k,t_n)$, given a radius r with $r \in \aleph$, $\forall\, t_n$ and $\forall\, z_k$, the vertical velocity is evaluated on an area of $(2r+1)^2$ grid points, i.e. the following samples are considered:

$$w(x_{i+s}, y_{j+s}, z_k, t_n) \quad with\ s = -r,...,r \tag{6}$$

If at least $(2r+1)^2/2+1$ grid points present a velocity greater than a threshold w_T, then:

$$w(x_i, y_j, z_k, t_n) = w(x_i, y_j, z_k, t_n) \tag{7}$$

otherwise:

$$w(x_i, y_j, z_k, t_n) = 0 \tag{8}$$

So, if ε in $P(x_j,y_i,z_k)$ at $t=t_n$ is evaluated according to (2), the integral in (1) can be discretized with the rectangle rule as follows:

$$LPI_{(x_i,y_j,t_n)} = \frac{1}{\left(z_{1_{i,j,n}} - z_{N_{k_{i,j,n}}}\right)} \frac{1}{4r^2} \sum_{k=1}^{N_{z,i,j,n}} \sum_{s=-r}^{r} \sum_{s=-r}^{r} [\varepsilon(x_{i+s}, y_{j+s}, z_k, t_n) \cdot ... \\ ... \cdot w^2(x_{i+s}, y_{j+s}, z_k, t_n) \cdot (z_k - z_{k-1})] \tag{9}$$

III. Model Setup and Observed Data

A. Model Setup

The Advanced Research Weather Research and Forecast model (WRF-ARW) V.3.4.1 is a fully compressible and non-hydrostatic model with a terrain-following vertical coordinate. The meteorological events analyzed are the Genoa's flood on 9 October 2014 and six ordinary events occurred in Switzerland. The different case studies have similar setup. For both cases two nested domains of 5 km x 5 km and 1 km x 1 km grid spacing have been used to cover the upper and lower limits of the cloud-permitting range. The analyses in this work have been done on the inner domain composed of 475x475 grid points for the Italian case and 246x360 grid points for the Swiss cases. The vertical levels are 83 and cover a height of 20 km. As microphysics parameterization, the WRF Single-Moment 6-Class Scheme (WSM6) [16] is used. This microphysics scheme is taken into account since ice species processes are modeled and as mentioned earlier, they are of particular relevance in the lightning activity.

The grid spacing range chosen for the two domains (5 and 1 km) makes the model able to solve explicitly, albeit crudely, many convective processes, then an explicit treatment of convective processes is chosen for this case. Each numerical simulation is initialized at 00UTC of the day of interest and initial and boundary conditions for the WRF simulations are provided by the European Centre for Medium-Range Weather Forecast (ECMWF) through Integrated Forecast System (IFS) that is a global model that runs every 12 hours.

B. Observed Data

Before starting with the analysis it is necessary to validate the numerical simulations of the considered events by comparing the predicted rainfall with the measured one. For the Italian case study, even though the Liguria territory is monitored by a significant number of rain gauges, they don't cover the area over the sea where most of the lightning discharges have been recorded for this event. Thus, radar data from the C-band polarimetric radar located at Monte Settepani in Savona (Italy) have been chosen since its data cover all the area of interest. Instead, for the Swiss case studies, MeteoSwiss rain gauges data have been chosen from the SwissMetNet database. It has actually about 130 automatic measurement stations that provide data every 10 minutes: for the prescribed case studies, 87 rain gauges in common for all the events have been selected.

Furthermore, in order to assess the LPI effectiveness, it is necessary to have at our disposal the lightning observed data corresponding to all the analyzed events. Since LPI is the measure of the potential for charge generation and separation that leads to total lightning occurrence, the total lightning obtained by taking into account both IC and CG flashes is used. The choice is supported also by the fact that both CG and IC flashes show an excellent correlation with updraft strength and with the timing of convective development [17]. For the Italian case study, the used data provide the position (longitude and latitude), an estimate of the lightning peak current (in kA) and the polarity of each lightning flash acquired by the LAMPINET lightning network of the Aeronautic Meteorological Service based on VAISALA technology. 15 sensors compose LAMPINET network and its detection efficiency is estimated to be 90% for lightning current peaks greater than 50 kA, and has a mean location accuracy over Italy and surrounding area of 500 meters [18]. For the Swiss case studies, the EUCLID (EUropean Cooperation for LIghtning Detection) data network has been used. EUCLID (European Cooperation for Lightning Detection) [19] is a consortium of 19 national lightning detection networks. EUCLID is characterized by an overall flash detection efficiency of 98% and stroke detection efficiency of 84% [20].

To compare these punctual observed lightning data with the maps of LPI, which are calculated on the WRF model grid, observed lightning data have been associated with the closest grid point of the model and assigned to the time range containing the exact lightning flash time.

IV. Application of the LPI

A. Italian Case Study

The high impact weather event, which hit the Genoa city on 9th October 2014, had the same back-building process observed during other events occurred in Liguria region in October 2010, October and November 2011 [21]. All these events showed that the area of intense precipitation swept an arc of a few degrees around the main trajectory assuming a v-shaped form. The Genoa 2014 event has been characterized not only by extreme rainfall depths (≈400 mm of daily precipitation in the central part of the Bisagno

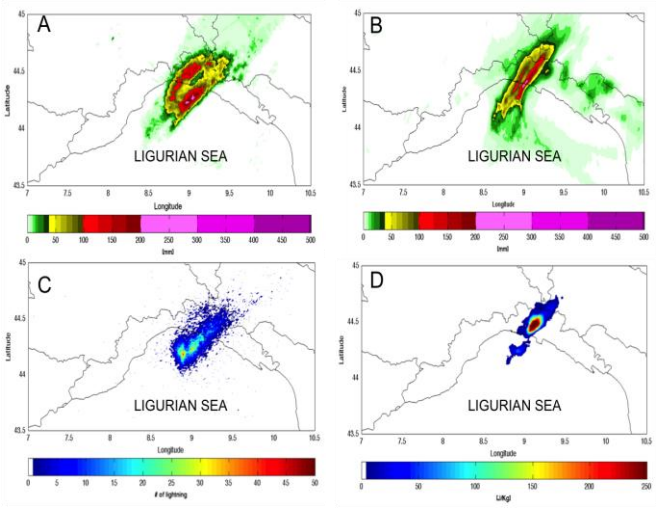

Figure 1. From 00 UTC to 12 UTC on October 9th 2014: QPE (panel A), QPF (panel B), LPI (panel D) and observed lightning (panel C).

catchment, with hourly peaks of about 150 mm), but also by an intense lightning activity; consequently it is worth analyzing the LPI behavior and its predictive ability for this case.

As previously stated, to assess the WRF model output reliability, a comparison between the quantitative precipitation forecast (QPF) obtained by the model with the quantitative precipitation estimation (QPE) from radar is necessary. During the morning the model gives a better representation of the reality with respect to the afternoon in terms of quantitative precipitation, so the LPI is calculated on that time window.

In terms of quantitative precipitation, it is possible to see in Fig. 1 (panels A and B) that the WRF model and the observed data are in a good agreement with a slight underestimation of the simulation results in terms of area swept by intense precipitation. The lightning activity predicted by the model (panel D) is more shifted on the ground with respect to the observations (panel C) that shows that the majority of lightning events has occurred on the sea. To investigate the reasons of this discrepancy, vertical sections of the modeled *w* field (not shown) have been done. This analysis has allowed to show that the WRF model predicts a smaller amount of vertical velocity over the sea with respect to the real strong convection responsible for the observed intense lightning activity. So since *w* is not high enough to overcome w_T, that grid point is not taken into account in the LPI estimation. The discrepancy between LPI predictions and the observed lightning data shows how important is the convection in the physical mechanism which generates lightning. Furthermore, this case suggests that the LPI is a good lightning forecasting tool whenever its input data, coming out of the meteorological model, are in good agreement with the observations.

B. Swiss Case Studies

While the first case analyzed was over a complex terrain near the sea in Italy, the other six study cases are over a complex topography in the Alps region in Switzerland. Here only two events in different seasons are presented to evaluate the LPI performance: the first is on June 22nd 2011 and the second is on December 14th 2011. The four events not shown here have similar results to the two presented cases.

For the first Swiss case, Fig. 2 shows as the model approximates quite well the observed lightning. The main difference with the Genoa case is the fact that the LPI map here (panel D) is not uniform in space. In particular, it is interesting to investigate why the LPI assumes values different from zero on the wind side (French side) of the Jura Mountains with respect to the observed data that are mainly located on the Swiss Plateau and Prealps (Fig. 3 panel G). A possible physical explanation is that mountainous regions generate gravity waves due to the interaction of thunderstorm clouds with orography. To better understand the gravity waves development, vertical sections of the *w* field have been analyzed at 14 UTC on the French and Swiss side of Jura mountain respectively (Fig. 3 in panels C and F). They show that the model predicts the presence of a stronger vertical velocity upward component on the French side of Jura (panel C) than on the Swiss side (panel F). This is due to the fact that a smoothed representation of orography in the model modifies the wind intensity: it generates more intense updrafts on the wind side of mountains with respect to the lee side of it. Since this type of updraft is not purely related to convection, i.e. it is not directly linked to a thermo-dynamical effects, it does not generate an intense lightning activity (panels A and D). Since the LPI formulation starts from the upward component of the vertical velocity, no matter its physical meaning, the result of (9) is an intense lightning activity wherever such speed assumes higher values (panels B and E).

The second case study in the Swiss territory corresponds to a very intense snowing day. Usually snowing process is not associated with strong convection, so a low lightning activity is expected to occur. Also in this case the LPI is applied in the second part of the day. Fig. 4 shows that there is an overestimation of the QPF with respect to the observed

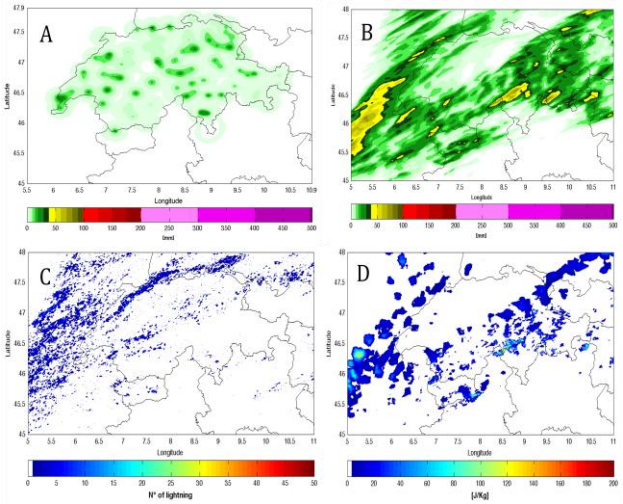

Figure 2. From 12 UTC to 24 UTC on June 22nd 2011: QPE (panel A), QPF (panel B), LPI (panel D) and observed lightning (panel C).

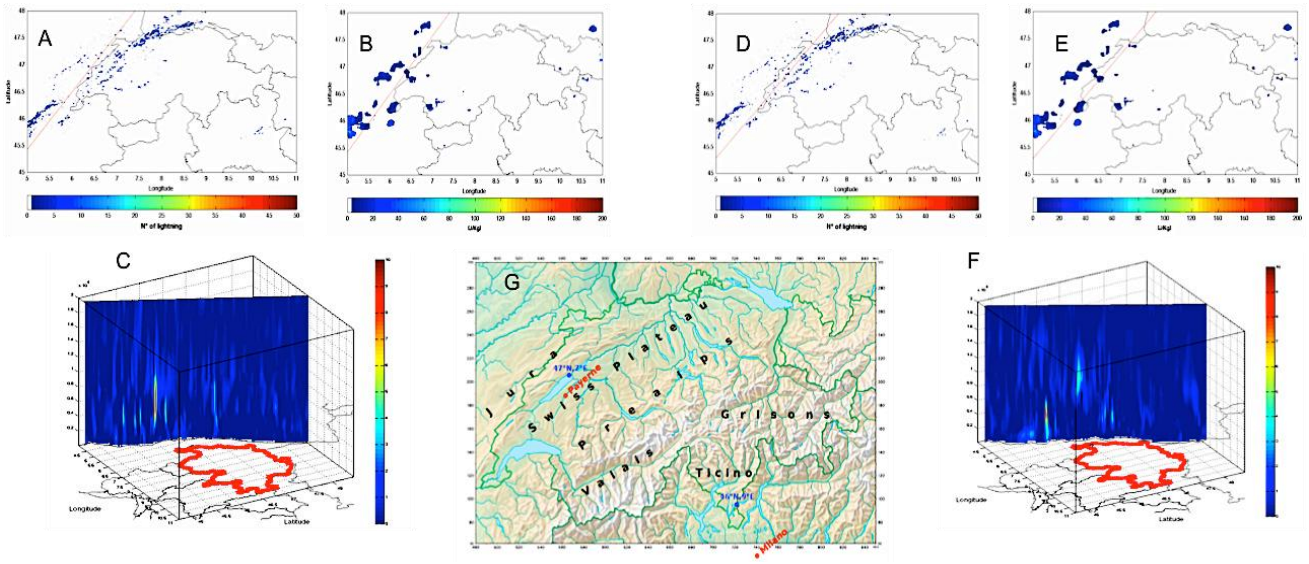

Figure 3. Observed total lightning (panel A and D) and LPI map (panel B and E) at 14 UTC on June 22nd 2011 with the projection of the vertical section in red. Vertical sections of the *w* velocity field on the French (panel C) and Swiss side (panel F) of Jura mountains with the Switzerland boundaries in red. Panel G represents the Switzerland terrain.

rainfall depth, and an overestimation of the observed lightning activity by the LPI. As previously done for the first Swiss case, vertical section of the *w* field is presented (Fig. 5 panel C) to investigate the reason of LPI presence despite observed data and meteorological conditions suggesting the absence of strong convection. Due to the fact that lightning occurrence depends not only on the presence of convection but also on the mixed phase moisture (represented by the ε function in the LPI formulation) that determines the conditions for charge generation and separation, a vertical section of the ε function is presented for this case (Fig. 5 panel D). Examining panels C and D, a possible explanation of the aforementioned overestimation could be the presence of both *w* and ε in the model results, while, during the event, the mixed phase moisture was not present in big quantity or the vertical velocity was not so strong. As a general comment, since the LPI is a post processing application that is imputed to the meteorological model outputs, two error sources have to be taken into account. The first one is related to the ability of the meteorological model in reproducing the real event; in other words, if the meteorological model makes some mistakes in the prediction of the vertical velocity and the microphysics species, the LPI formula will be fed with incorrect input data and so will not be able to represent the lightning activity in a satisfactory manner. This aspect is evident in the exam of the Italian case. The second possible source of uncertainties is related to the LPI formulation. The Swiss cases suggests that a formula which relies on the upward velocity without making any specification on the related physical process can fail whenever the presence of such velocity is not connected with a strong convection and

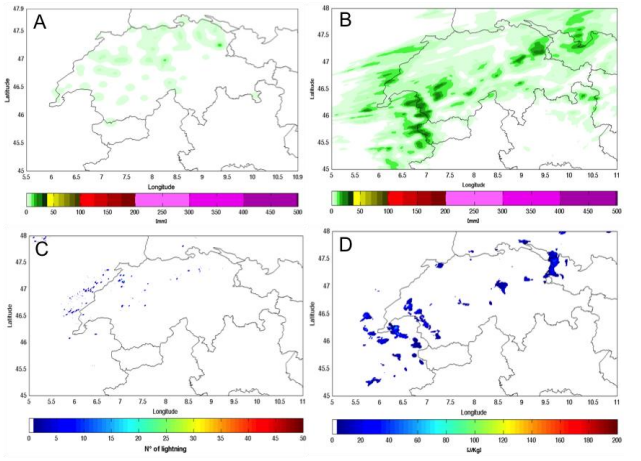

Figure 4. Comparison between QPE (panel A) and QPF (panel B) and between observed lightning activity (panel C) and LPI map (panel D) from 12.00 UTC to 24.00 UTC on December 14th 2011.

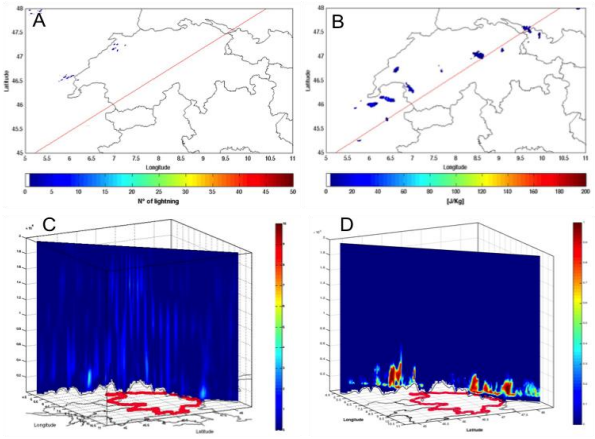

Figure 5. Vertical section of the w upward component (panel C) and of epsilon function of LPI formula (panel D). Representation of the projection of the section (red line) on the observed total lightning (panel A) and on the LPI map (panel B) at 15.00 UTC.

whenever there is the presence of the mixed phase moisture in the model simulation that is not present in the real event.

V. CONCLUDING REMARKS

The paper has presented the definition, the implementation and the application of the LPI to different case studies to test its behavior in different complex topographic conditions: one case is on an Italian sea place (Liguria region), while the other six are ordinary events in the Swiss territory. The Italian case study is relative to a high impact weather event occurred on 9th October 2014, characterized by a huge quantity of precipitation and an intense lightning activity. On the other hand, the events chosen in Swiss aren't characterized by heavy rain, but they are important to evaluate the LPI on a complex terrain in different seasons. The LPI in the Genoa case has revealed to be a good approximation of the observed lightning activity whenever the model can reproduce the convective process on the sea area where lightning activity is observed. The main problem in the LPI estimation seems to be linked to the model difficulty in correctly reproducing the convective field that characterized the event. However, it can be considered as a good forecasting tool coupled with the rainfall prediction, because it shows a very high potential in an area quite correct with respect to the localization of the observed torrential rainfall. For the Swiss cases, the LPI assumed a spot shape with respect to the homogeneous potential given in Genoa case study. This behavior is probably due to the passage of the thunderstorm over the mountains that can produce updrafts and downdrafts. This particular behavior is highlighted in winter snowing events that usually aren't characterized by strong convection, while the model predicts significant vertical velocity fields that result in high LPI values. Future work will concern the possibility of testing the LPI effectiveness in areas characterized by geographic configurations subjected to different types of atmospherical processes or use a multi-physics ensemble approach for a probabilistic LPI estimation. Another possible research line could be relevant to the formulation of different indices and to compare their performances with the LPI one.

ACKNOWLEDGMENT

This work was supported by the Italian Civil Protection Department and by the Ligurian Environmental Agency. Thanks are due to EUCLID group for the lightning observations for Switzerland provided and to LRZ Supercomputing Centre, Garching, Germany, where the numerical simulations were performed on the SuperMUC Petascale System, Project-ID: pr45de.

REFERENCES

[1] International Strategy for Disaster Reduction (ISDR), "Natural disasters and sustainable development: understanding the links between development, environment and natural disasters," United Nations international strategy for disaster reduction. United Nations Publications Centre, Geneva, 2002.

[2] Intergovernmental Panel on Climate Change (IPCC), "Climate change 2014: Mitigation of Climate Change," World Meteorological Organization (WMO) and UN Environment Programme (UNEP), 2014.

[3] W. Deierling and W. A. Petersen, " Total lightning activity as an indicator updraft characteristics," J. Geophys. Res., vol 113, D16210, doi:10.1029/2007JD009598, 2008.

[4] C. P. R. Saunders, "Charge separation mechanisms in clouds," Space Sci. Rev., vol 137 (1-4), pp. 335-354, doi:10.1007/s11214-008-09345-0, 2008.

[5] C. G. Price, "Lightning application in weather and climate research," Surveys in Geophysics, vol 34(6), pp 755-767, 2013.

[6] S. Soula, S. Chauzy, "Some aspects of the correlation between lighning and rain activities in thunderstorms," Atmos. Res., vol 56, pp 355-373, 2001

[7] C. G. Price and B. Federmesser, "Lightning-rainfall relationships in Mediterranean winter thunderstorms," Geophys. Res. Letters 33, doi: 10.1029/2005GL024794, 2006.

[8] C. Adamo, S. Goodman, A. Mugnai, J.A. Weinman, "Lightning measurements from satellites and significance for storms in the Mediterranean. In: Betz HD, Schumann U, Laroche P (eds) Lightning: principles, instruments and applications. Review of modern lightning research. Springer, Berlin, pp 309–329.

[9] B. Lynn and Y. Yair, "Prediction of lightning flash density with the WRF model," Adv. Geosci., vol 23, pp 11-16, 2010.

[10] E. W. McCaul, S. Goodman, K. M. LaCasse and D. J. Cecil, "Forecasting lightning threat using cloud-resolving model simulations," Wea. Forecasting, vol 24, pp 709-729, 2009.

[11] J. M. L. Dahl, H. Holler and U. Shumann, "Modeling the flash rate of thunderstorms. Part I: Framework," Mon. Wea. Rev., vol 139, pp 3093-3111, 2011.

[12] B. Lynn and Y. Yair, "Lightning Potential Index: A new tool for predicting the lightning density and the potential for extreme rainfall," Geophys. Res. Abstracts, EGU General Assembly, Vienna, vol 10, 2008.

[13] Y. Yair, C. Price, V. Kotroni, K. Lagouvardos, E. Morin, A. Mugnai and M. d. C Llasat, "Predicting the potential for lightning activity in Mediterranean storms based on the Weather Research and Forecasting (WRF) model dynamic and microphysical fields," J. Geophys. Res., 115, D04205, 2010.

[14] E. R. Mansell, C. L. Ziegler, E. C. Bruning, "Simulated electrification of a small thunderstorm with two-moment bulk microphysics," J. Atmos. Sci., vol 67, pp 171-194, 2010.

[15] M. S. Van den Brooke, D. M. Schultz, R. H. Johns, J. S. Evans, J. E. Hales, "Cloud-to-ground lightning production in strongly forced, low-instability convective lines associated with damaging wind," Wea. Forecasting, vol 20, pp 517-530, 2005.

[16] S.-Y. Hong and J.-O. J. Lim, "The WRF single-moment 6-class microphysics scheme (WSM6)," J. Korean Meteor. Soc., vol. 42, pp 129-151, 2006.

[17] C. J. Shultz, W. A. Petersen, L. D. Carey, "Lightning and severe weather: a comparison between total and cloud-to-ground lightning trends," Wea. Forecasting, vol. 26, pp. 744-755, 2011.

[18] L. De Leonibus, D. Byron, M. Sist, D. Labate, F. Zauli, D. Melfi, "Wind intensity reconstruction over Italy through lampinet lightning data," 3rd International Lightning Meteorology Conference, Orlando, Florida, 2010.

[19] G. Diendorfer, "EUCLID—technical structure and performance of the European wide lightning location system," Proc. Int. Conf. on Grounding and Earthing and 3rd Brazilian Workshop on Atmospheric Electricity, Rio de Janeiro, Brazil, 2002.

[20] Schulz, W., S. Pedeboy, C. Vergeiner, E. Defer, and W. Rison, Validation of the EUCLID LLS during HyMeX SOPI, International Lightning Detection Conference, Tucson, 2014.

[21] E. Fiori, A. Comellas, L. Molini, N. Rebora, F. Siccardi, D. Gochis, S. Tanelli and A. Parodi "Analysis and hindcast simulations of an extreme rainfall event in the Mediterranean area: The Genoa 2011 case". Atmos. Res., 138, 13-29, 2014.